Isotope effect on the E_{2g} phonon and mesoscopic phase separation near the electronic topological transition in $Mg_{1-x}Al_xB_2$

L. Simonelli,[1] V. Palmisano,[1] M. Fratini,[1] M. Filippi,[2] P. Parisiades,[3] D. Lampakis,[3] E. Liarokapis,[3] and A. Bianconi[1]
[1]*Department of Physics, Sapienza University of Rome, Piazzale Aldo Moro 2, 00185 Roma, Italy*
[2]*Laboratoire CRISMAT, UMR6508, 6 Boulevard Maréchal Juin, 14050 CAEN Cedex 4, France*
[3]*Department of Physics, National Technical University of Athens (NTUA), Zografou Campus, Athens GR157 80, Greece*
(Received 22 January 2009; revised manuscript received 8 May 2009; published 24 July 2009)

We report boron isotope effect on the E_{2g} phonon mode by micro-Raman spectroscopy on the ternary $Mg_{1-x}Al_xB_2$ system, synthesized with pure isotopes ^{10}B and ^{11}B. The isotope coefficient on the E_{2g} mode frequency is nearly 0.5 in the wide range of Al, with a tendency to decrease at MgB_2 ($x=0$). The intraband electron-phonon (e-ph) coupling relative to the sigma band has been extracted from the E_{2g} line-shape parameters. By tuning the Fermi energy near the electronic topological transition (ETT), where the sigma Fermi surface changes from two-dimensional to three-dimensional topology (in range $0<x<0.28$), the E_{2g} mode shows the Kohn anomaly accompanied with a splitting into a hard and a soft component. The results suggest that the intraband hardly plays any role to control the high T_c of $Mg_{1-x}Al_xB_2$ The common physical features of diborides with the multigap FeAs-based superconductors and cuprates are discussed.

DOI: 10.1103/PhysRevB.80.014520 PACS number(s): 74.62.Dh, 74.70.Ad, 78.30.Er

I. INTRODUCTION

High T_c superconductivity, where a macroscopic quantum condensate overcomes the decoherence effects of temperature, shows up in three different systems: cuprates, diborides, and iron pnictides. The physical features determining the common quantum mechanism for high T_c can be unveiled by the few common features:

first, they are multilayer materials made of active metallic layers (boron layers in *diborides*,[1,2] CuO_2 layers in *cuprates*,[3–7] and $FeAs_{4/4}$ layers in *iron pnictides*,[8,9]) separated by spacer layers. The active (spacer) layers contribute (do not contribute) to the electronic states at the Fermi level;

second, the high T_c phase shows up by fine tuning of the chemical potential in a regime where electronic states with different spatial distribution and/or symmetry coexist at the Fermi level, giving rise to an anisotropic multigap superconductivity;[7]

third, the high T_c phase occurs in a regime at the edge of mesoscopic phase separation (MePhS) with competing phases.

In all these systems (diborides,[2] cuprates,[6] and iron pnictides[9]) the chemical potential is tuned in the proximity of an electronic topological transition (ETT), where a phase separation is expected to occur in the presence of disorder.[10]

The high T_c superconducting diborides, where both the σ holes and π electrons coexist at the Fermi level, have been the first clear case of multiband anisotropic superconductivity [for a review see Ref. 7]. In this system the duality of the electron gas at the Fermi level is provided the σ electrons and the π electrons. In the MgB_2 ($T\sim 40$ K) the Fermi level in below the σ band edge breaking the standard BCS approximation of a large Fermi energy for the s holes, a small variation of the chemical potential moves the Fermi level near an electronic topological transition,[7,10] where the σ Fermi surface changes its dimensionality from two-dimensional (2D) to three-dimensional (3D), called a type (II) ETT.[7,9] While a strong electron phonon coupling with a Kohn anomaly (giving a phonon softening) is expected for the 2D Fermi surface topology,[11] a suppression of this coupling is expected in the 3D regime.

In the standard BCS superconductivity mechanism phonons couple to charge carriers to give the Cooper pairs. For the simplest case of a single effective phonon frequency ω involved in the pairing the McMillan's formula predicts $K_BT_c=\hbar\omega e^{\tilde{\lambda}}$. The isotope effect of superconducting critical temperature T_c is described in terms of the isotope coefficient (IC) α defined by the relation $T_c\propto M^{-\alpha}$ where M is the ionic mass. Under the assumption that the shift ΔT_c induced by isotopic substitution ($M\rightarrow M^*$) is small compared to T_c, one can write $\alpha=-\frac{M}{\Delta M}\frac{\Delta T_c}{T_c}$, *where* $\Delta M=M-M^*$ is the difference between the two isotopic mass. The presence of an isotope effect on the critical temperature T_c is usually considered to be a measure to the contribution of phonons to the pairing mechanism. In the simplest case (neglecting repulsive Coulomb pseudopotential, or the relative weight of different electron-phonon coupling strengths or the presence of magnetic impurities, or proximity effect or nonadiabaticity in the system, and finally magnetic or electronic pairing mechanisms) the isotope coefficient will be the same as the isotope coefficient on the phonon mode $\omega\propto M^{-\alpha_p}$ with $\alpha_p=0.5$, in the simple harmonic approximation.

Soon after the discovery of superconductivity in MgB_2, a finite boron isotope effect of T_c, measured by Bud'ko *et al.*[12] and Hinks *et al.*,[13] has been used as support for a phonon mediated superconductivity in the MgB_2.[14–16] Indeed a strong coupling of the B-B bond-stretching E_{2g} phonons to the $B2p\sigma$ hole bonding states (2D Fermi surface) has been assumed to be responsible for the remarkable superconductivity in MgB_2. However the measured isotope coefficient on the T_c is $\alpha\approx 0.3$, less than 0.5 that is the expected value in standard BCS superconductors with negligible Coulomb repulsion. Initially the reduction of the isotope effect was assigned to anharmonicity and the effect of Coulomb repulsion.[17] Recent experimental results and theoretical analysis indicate that anharmonicity plays only a marginal

role leaving the isotope effect as the most important unresolved issue in the physics of MgB_2.[18]

Various nonconventional mechanisms have been invoked so far for high T_c in diborides: bipolaron superconductivity,[19] and electronic mechanisms such as the resonating valence bond mechanism,[20] the electron-hole asymmetry,[21] the pairing mediated by collective electronic excitations,[22] charge density excitations.[23,24] A two component scenario has been proposed (including pairing mediated by acoustic plasmons[25,26]) where the key term for high T_c is the exchangelike interband pairing[27–29] i.e., the direct exchange of pairs between the two components with a "Feshbach resonance"[30–32] as discussed in Ref. 7. The Feshbach resonance can be described as the direct exchange of pairs of particles in a first band and pairs of particles in a second band, where the two bands differ for spatial locations, symmetry and intraband e-ph coupling. The exchange pairing has a Feshbach resonance where pairs in a large Fermi surface resonate with second pairs in a second band where the Fermi level is near an ETT.[7] The system will show a crossover from a BCS-like to Bose-like scenario where the bipolaron states in the second band are degenerate with the Fermi level in the first band. Therefore in diborides the high T_c would be controlled by the exchangelike interband pairing between the strongly bound hole pairs in the σ band (that could be described as bipolarons formed by the large phonon mediated intraband pairing) and the electron pairs in the π band, In this proposal the variation of the electron phonon coupling in the intraband pairing in the σ band is very important but the exchange pairing is expected to be the driving term raising T_c.

The experimental method to test these theoretical models is to measure the response of the superconducting phase tuning the chemical potential. In fact the electron-phonon coupling is strongly sensitive to the relative position of the chemical potential and the ETT in the σ band.[11] The first method that enabled tuning the chemical potential has been the external pressure. The response of the system to pressure has provided experimental evidence of the proximity to an ETT.[33] The second method has been the chemical substitution in the spacer layers, but unfortunately substitutions in the Mg site appeared to be difficult, in many case unsuccessful or ambiguous. The most successful of these attempts is the Al substitution for Mg, reported by several groups,[34–42] that allows the tuning of the chemical potential from above to below the edge of the σ band, while changing the superlattice misfit strain between the hcp Al/Mg layers and the honeycomb boron layers that can be measured via the tensile microstrain in the boron lattice.[1]

It is now well established that the $Mg_{1-x}Al_xB_2$ ternary system is a two-band and two-gap superconductor[43–47] where the T_c decreases by increasing the Al content from 40 K in MgB_2 to the disappearance of superconductivity for $x=0.57$. The E_{2g} phonon frequency shows a large softening going from AlB_2 to MgB_2.[48–51] The theoretical calculation of the electron-phonon interaction as a function of x has been presented by several authors[52,53] and the evolution of the electronic structure with x has been probed by x-ray absorption and optical spectroscopy.[54]

A key point of the physics of the high T_c superconductivity in diborides is that MgB_2, where the highest T_c is reached, is at the edge of a catastrophe. In fact for small variations of the chemical potential[34] or pressure[33] the system shows a structural phase separation. For example in the case of aluminum for magnesium substitution a first structural phase separation region is detected by x-ray diffraction (XRD) in the range $0<x<0.25$ detected in the early times[34] has been well confirmed by high resolution x-rays diffraction.[2] However in this range of doping the transport data[55] show a single superconducting phase with a single critical temperature indicating that the structural phase separation occurs on a smaller scale than the superconducting coherence length.

In this work we have investigated a very large number of $Mg_{1-x}Al_x\ ^{10}B_2$ and $Mg_{1-x}Al_x\ ^{11}B_2$ samples[2] using micro-Raman spectroscopy to investigate the evolution of electron-phonon interaction and the phase separation with Al doping. We have investigated the isotope pure samples as a function of chemical potential to detect a possible anomaly of the isotope coefficient on the phonon frequency α_p and the variation of E_{2g} phonon line-shape in order to detect: (1) the phase separation observed in high resolution x-ray diffraction but not in the superconducting critical temperature and (2) the evolution of electron-phonon interaction.

We show here that the E_{2g} phonon frequency follows the harmonic mass law in almost all the Al content range ($0<x<0.57$). The maximum T_c is found to be at the boundary of a mesoscopic phase separation and decreases entering in the phase separation regime. The extracted electron-phonon coupling strength as a function of x shows a large increase where the chemical potential is tuned near the type (II) ETT, on the contrary it shows negligible variations where the chemical potential is tuned near the type (I) ETT in the sigma band. The results suggest that the intraband electron-phonon mechanism is not the only term controlling the high T_c superconductivity in the diborides, in contrast to the commonly accepted assumption that the T_c is mainly determined by the electron-phonon pairing strength in the sigma band.

II. EXPERIMENTAL METHODS

We have synthesized several polycrystalline samples in a wide range of Al content, from the pure MgB_2 to the ternary system with $x=0.57$, by direct reaction method of the elemental magnesium, aluminum, and boron ($^{10}B/^{11}B$) (Eagle Picher 99% purity).[55] The starting powders were mixed in the stoichiometric ratio and pressed into a pellet. The pellets were enclosed in a tantalum crucible, sealed by arc welding under argon atmosphere, and then heated for 1 h at 800 °C and 2 h at 950 °C. The samples have been cooled to room temperature with a 4 K/m rate. Several pieces in each pellet were analyzed by XRD to look for any Al gradient or extrinsic inhomogeneities. We have obtained a very good reproducibility of the samples with no extrinsic inhomogeneities. The superconducting properties of all the samples were investigated by susceptibility measurements.

We have collected micro-Raman spectra on the isotopically substituted samples. The Raman spectra have been measured in the back-scattering geometry, using a T64000 Jobin-Yvon triple spectrometer with a charge-coupled device

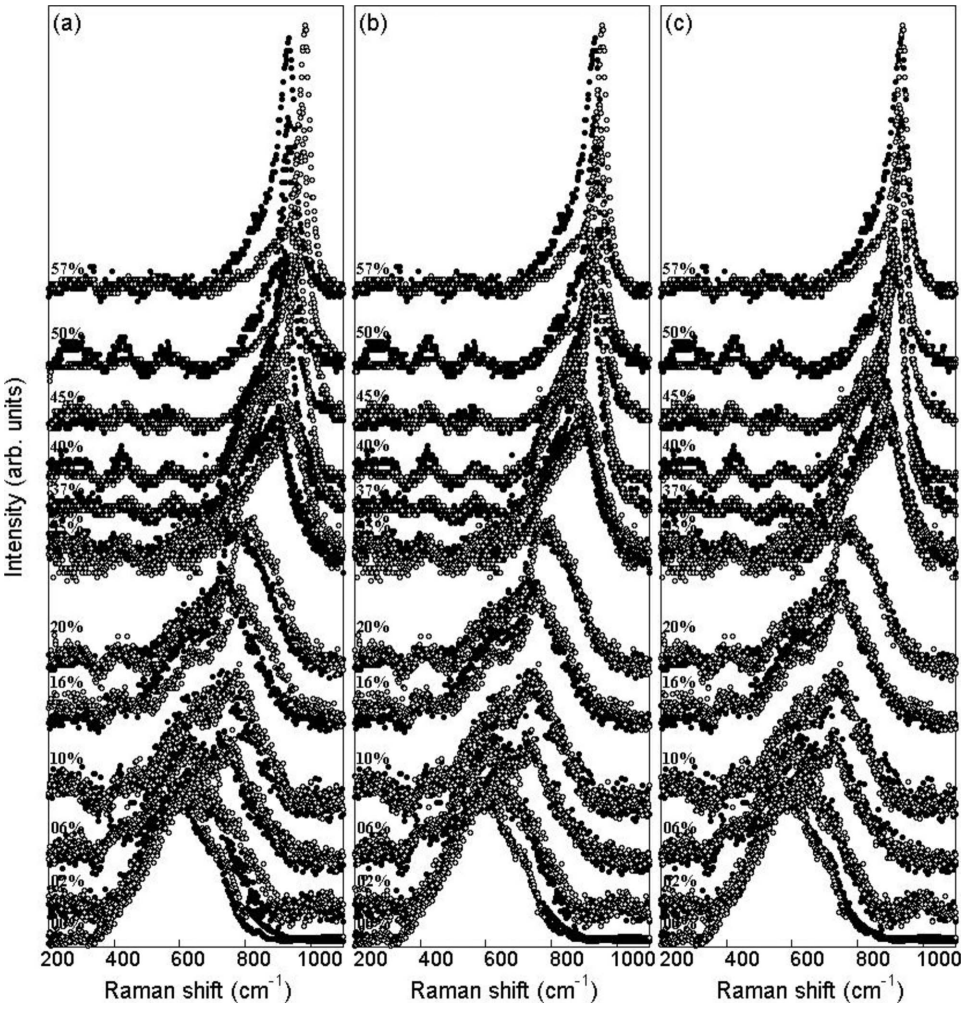

FIG. 1. Comparison between Raman spectra on $Mg_{1-x}Al_x$ $^{11}B_2$ (filled dots) and $Mg_{1-x}Al_x$ $^{10}B_2$ (open symbols) samples for $0<x<0.57$ (panel a). The energy scale of the Raman spectra of $Mg_{1-x}Al_x$ $^{10}B_2$ (filled dots) is multiplied by the factor $(10/11)^{0.3}$ (panel b) and by the factor $(10/11)^{0.5}$ (panel c).

camera. The explored Raman shift range is between 50 and 1200 cm^{-1}. The 488.0 and 531.1 nm laser lines have been focused on 1–2 μm large crystallites and the power was kept below 0.1 mW to avoid heating by the beam. For each sample several measurements have been performed on different microcrystallites choosing different region of the samples. The spectra have been collected at room temperature in a wide range of Al content ($0<x<0.57$).

III. RESULTS AND DISCUSSION

The micro-Raman spectra of $Mg_{1-x}Al_x$ $^{11}B_2$ (filled dots) and $Mg_{1-x}Al_x$ $^{10}B_2$ (open symbols) samples are reported in Fig. 1(a) after background subtraction. A clear phonon isotope shift is observed. To visualize the shift properly we plot the spectra of $Mg_{1-x}Al_x$ $^{10}B_2$ samples as a function of Raman shift multiplied by the factor $(10/11)^{0.3}$ in panel (b) of Fig. 1 in order to compare the isotope shift of the Raman active phonon with the isotope shift of the superconducting critical temperature in pure MgB_2 showing an isotope coefficient 0.3.[12,13] In panel (c) the spectra of $Mg_{1-x}Al_x$ $^{10}B_2$ samples are plot as a function of Raman shift multiplied by the factor $(10/11)^{0.5}$ according to the harmonic mass law. The spectra for the two isotopically substituted sample sets are almost coincident in Fig. 1(c), showing that the Raman response to isotopic substitution scales according to the harmonic mass law, with a slight deviation at very low Al content.

In the data it is possible to distinguish two phonon components: the Raman active E_{2g} in-plane stretching mode of the boron atoms, and the silent B_{1g} activated by disorder that involves vibrations of the boron atoms along the off plane direction. Increasing the Al content the structural disorder increases[2] enhancing the contribution of the B_{1g} mode to the Raman spectra. At the same time, we observe a linewidth narrowing and energy hardening of the E_{2g} mode with increasing Al substitution, in agreement with previous results.[48–50] In the range $0<x<0.28$ the E_{2g} mode split into two E_{2g} contributions (a hard mode and a soft mode) induced by the mesoscopic phase separation,[2] in agreement with diffraction data showing the splitting of the c axis.[2]

The Raman spectra have been fitted with a three component model to represent the B_{1g} and the two (soft and hard) E_{2g} components, as it is shown in Fig. 2. The relative weight of the soft and hard E_{2g} components has been reported in Fig. 12a of Ref. 2. In Fig. 3(a) we report the evolution of the values of the E_{2g} phonon frequency as a function of Al content for samples synthesized with ^{10}B (open symbols) and ^{11}B (filled dots) and their weighted average (solid, ^{11}B, and dashed, ^{10}B, line) of the energy of the E_{2g} phonon, with the weighting given by the relative intensities of the "hard" and "soft" components. Figure 3(b) shows the isotope shift in-

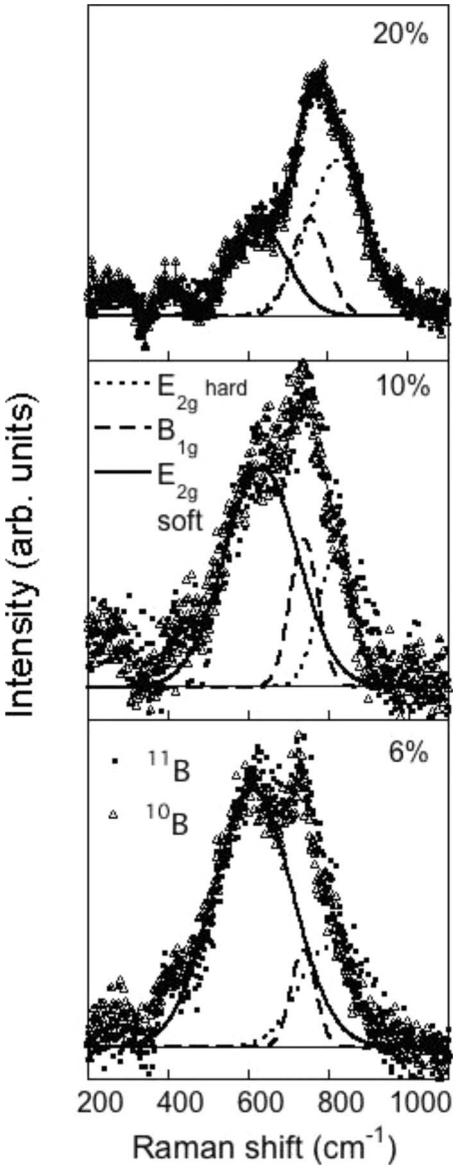

FIG. 2. Typical fit with three components of the Raman data of $Mg_{1-x}Al_x$ $^{11}B_2$ (filled dots) and $Mg_{1-x}Al_x$ $^{10}B_2$ (open symbols) samples (the Raman shift of $Mg_{1-x}Al_x$ $^{10}B_2$ is multiplied by the factor $\sqrt{10/11}$). The dashed lines represent the B_{1g} contribution, the solid line the soft E_{2g} contribution and the dotted line the hard E_{2g} contribution for aluminum concentration 20%, 10%, and 6% showing the increasing intensity of the hard E_{2g} component with increasing Al concentration.

duced on the E_{2g} phonon $\alpha_p = \ln(\omega_{10}/\omega_{11})/\ln(11/10)$ hard and soft frequencies between samples synthesized with different isotopes of boron. The phonon isotope coefficient plotted as a function of x, shows that the average phonon isotope coefficient is $\alpha_p = 0.5$ within the error bars in the full Al substitution range. However the data for the soft mode show some possible deviations at very low doping, in fact there the error bars are much larger and the data could be consistent also with a phonon isotope coefficient as small as $\alpha_p = 0.3$ at very low Al doping.

The E_{2g} phonon mode undergoes a substantial variation in terms of a weighted average, with the weighting given by the

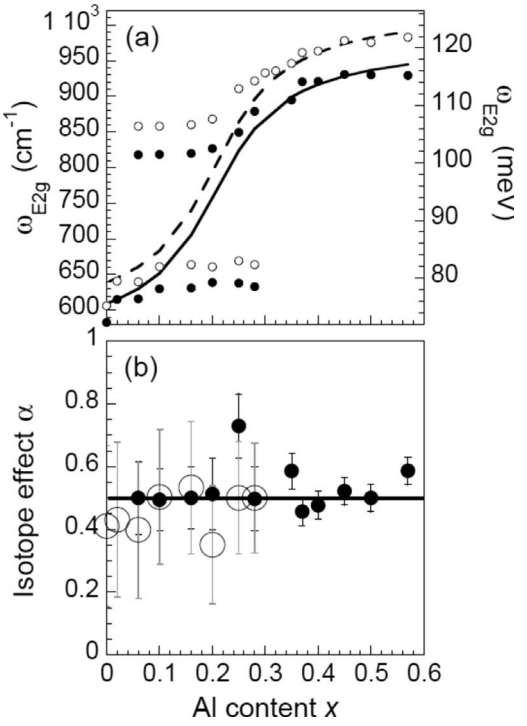

FIG. 3. (Panel a) The frequency of the hard and soft components of the E_{2g} mode for ^{10}B (open circles) and for ^{11}B (filled dots) is reported. The energy hardening of the E_{2g}-mode with increasing Al substitution is shown. The splitting of the hard and soft E_{2g} mode (phase separation) occurs between 0% and 25% of Al content. The weighted average of the E_{2g} frequency weighted by relative intensity of the "hard" and "soft" components are plotted for the ^{11}B systems (solid line) and ^{10}B systems (dashed line). (Panel b) The isotope coefficient of the phonon mode as a function of x. The open symbols correspond to the low energy (soft) mode, while the filled dots to the high energy (hard) mode.

relative intensities of the "hard" and "soft" components, of the frequency [Fig. 3(a)] and width [see Fig. 11b in Ref. 2] below 28% of Al content. The investigation of a large number of samples allows us to identify the phase separation regime between 0% and 28% of Al content indicated by the splitting of the E_{2g} mode below $x = 0.28$ in a hard and a soft mode with the relative probability plotted in Fig. 3(b).

The linewidth of the profiles of the soft and hard E_{2g} Raman lines, in the phase separation regime, show a full width at half maximum (FWHM) around 200 and 150 cm^{-1}, respectively. So while the width decreases abruptly out of the phase separation region where the topology of the σ Fermi surface is 3D. The relative probability of the two E_{2g} contributions [Fig. 12(a) in Ref. 2] shows that the weight of the soft E_{2g} mode decreases on increasing the Al content, while the weight of the hard E_{2g} mode increases. The phase separation indicated by the splitting of the Raman E_{2g} mode is in agreement with the phase separation identified by the splitting of the (002) reflection peak in the x-ray diffraction data reported recently[2] confirming the early results.[34] Goncharov *et al.*[33] have shown that a similar phase separation is induced by nonhydrostatic pressure. They have studied the variation of the Raman spectra and x-ray diffraction data applying either a hydrostatic or a nonhydrostatic pressure on MgB_2.

Applying the nonhydrostatic pressure they have found a splitting of the Raman E_{2g} mode, together with a splitting of the (002) XRD reflections peaks. Therefore we can deduce that the variation of the chemical pressure induced by the Al substitution for Mg induces a similar effect as nonhydrostatic pressure. The substitution of Al for Mg in the spacer layers intercalated between the superconducting boron layers changes the misfit strain between the two types of layers forming the superlattice. Therefore we can conclude that the variation of the misfit strain has a similar effect on the splitting of phonon modes as the nonhydrostatic pressure.

In $Mg_{1-x}Al_xB_2$ we observe the splitting of the phonon mode but we have not been able to detect the splitting of the superconducting transition into two different critical temperatures[55] in agreement with previous works,[34,39,44,56,57] therefore we can identify the present phase separation as a mesoscopic phase separation forming a granular superconductor.

Let us now compare the present results with the case of the $Mg_{1-x}Sc_xB_2$ system showing the macroscopic phase separation in the range $0<x<0.1$.[58] In this case for $x>0.13$ the σ Fermi surface has a 3D topology and the Kohn anomaly is suppressed as indicated by the hardening and narrowing of the E_{2g} phonon mode. In this case the chemical substitution of Sc^{3+} for Mg^{2+} ions induces a variation of the chemical potential (the charge transfer between different layers) but since the Mg^{2+} and Sc^{3+} ions have the same ionic radius the misfit strain remains constant. Therefore the Sc substitution changes the charge density with a minimum lattice disorder. In the case of $Mg_{1-x}Sc_xB_2$ we observe a splitting of the superconducting critical temperature indicating two different material phases with different T_c (Ref. 58) and therefore we can conclude that there is a macroscopic phase separation.

The phase separation occurring where the chemical potential is driven at the type (II) ETT in the boron layers is determined by the presence of two types of local perturbations in the spacers: (a) the local random coulomb fields, determined the random distribution of ions with different ionic charge (Al^{3+} and Mg^{2+}) and (b) the local lattice distortions due to coexistence of ions with different ionic radius. Therefore the large miscibility gap[58] around the ETT in the case of $Mg_{1-x}Sc_xB_2$ between $x=0$ and $x=0.15$ with the formation of a macroscopic phase separation between the $x=0$ and the $x=0.15$ phase is associated with the case where the role of the local random Coulomb fields is dominant while role of the local lattice distortions is negligible. On the contrary the mesoscopic phase separation observed here, in the $Al_xMg_{1-x}B_2$ system, is associated with the case where both the local lattice distortions in the spacer layers, acting as point impurities for the elastic strain field, and charge impurities, acting as sources of the random coulomb fields for charge ordering, are of relevance.

The variation of the strength of the intraband electron-phonon coupling (e-ph) can be extracted from the E_{2g} softening[15] and linewidth narrowing.[11] The E_{2g} softening as a function of x has been predicted by different authors.[52,53,59] Taking into account that transport data show a single critical temperature in we have related T_c with a weighted average of the energy of the E_{2g} phonon, with the weighting given by

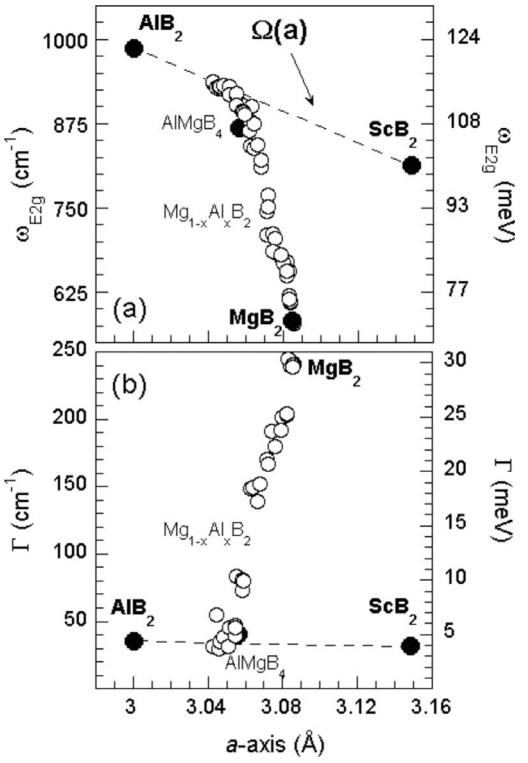

FIG. 4. (a) Energy of the E_{2g} mode as a function of the a axis going from the AlB_2 to MgB_2 samples. The dashed line shows the expected behavior due to lattice expansion for a metallic covalent material. The open circles represent the weighted average energy of the E_{2g} mode for the Al *doped system.* (b) The linewidth of the E_{2g} phonon mode as a function of the a-axis. The open circles represent the weighted average of the E_{2g} linewidth for the Al *doped system.*

the relative intensities of the "hard" and "soft" components. The weighted average of the energy (panel a) and the FWHM (panel b) of the E_{2g} phonon are plotted in Fig. 4 as a function of the a axis measured by x-ray diffraction in fact the phonon energy is expected to shift with the in-plane lattice compression. The variation of the E_{2g} mode $\Omega(a)$ due only to the lattice compression for a covalent material in the absence of anomalous electron-phonon coupling variations is shown in Fig. 4(a) by a dashed line $\Omega(a)$. The anomalous large e-ph coupling between the σ holes and the optical E_{2g} phonon can be derived from the ratio between the square of the expected linear behavior $\Omega(a)$ and the square of the measured frequency that is plotted in Fig. 5(a) as a function of a axis.

Moreover the e-ph coupling is related with the ratio between the full width at half maximum Γ and the energy of the E_{2g} mode reported in Fig. 5(b). The frequency hardening and the linewidth narrowing of the Raman E_{2g} mode indicates a clear decrease of the electron-phonon intraband coupling in the σ band going from MgB_2 to the doped samples.

The experimental softening of the E_{2g} mode is reported as a function of Al substitution in Fig. 6(a) in order to compare the experimental results with the predicted softening based on phonon and electronic band structure calculations of Profeta *et al.*,[52] Zhang,[53] and De la Peña-Seaman *et al.*[59] The results show that there is clear disagreement between the

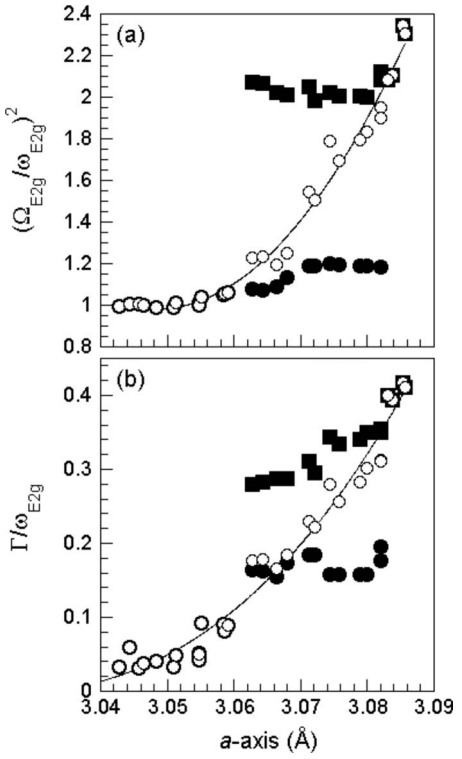

FIG. 5. (a) Ratio between the expected frequency due to the variation of the lattice compression and the measured E_{2g} phonon frequency as a function of the a axis in the $Mg_{1-x}Al_xB_2$ system. (b) Ratio between the linewidth and the energy of the E_{2g} phonon mode as a function of a axis. The black squares correspond to the soft E_{2g} contribution, while the black disks to the hard E_{2g} contribution. The calculated mean values are reported in open circles.

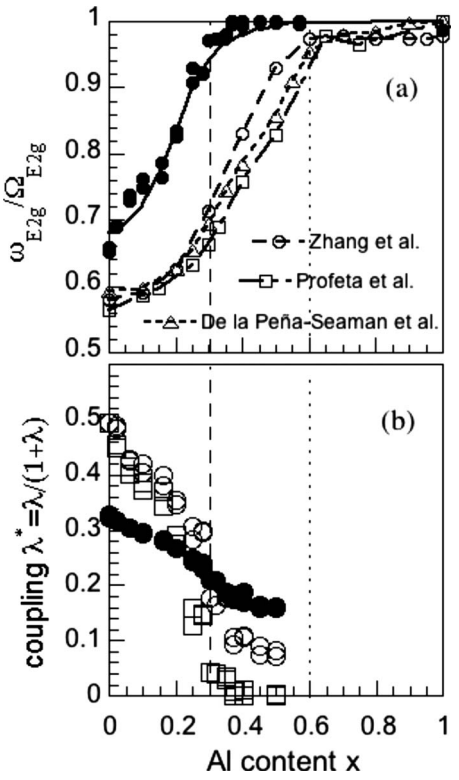

FIG. 6. (a) The measured E_{2g} phonon frequency $\omega_{E_{2g}}$ normalized for the frequency shift due to lattice a-axis compression $\Omega_{E_{2g}}$ in the $Mg_{1-x}Al_xB_2$ system (filled dots). The experimental softening of the E_{2g} mode frequency as a function of Al substitution is compared with calculations of Profeta *et al.* (Ref. 52) (open squares), Zhang *et al.* (Ref. 53) (open circles), and De la Peña-Seaman *et al.* (Ref. 59) (filled triangles) (b) The electron-phonon coupling $\lambda^*=\lambda/(1+\lambda)$ calculated from the softening (Ref. 15) (open circles) and widening (Ref. 11) (open squares) of the E_{2g} mode. The experimental effective coupling $-1/\ln(K_BT_c/\hbar\omega_{E_{2g}})$ (filled circles) obtained from the ratio between the superconducting critical temperature T_c measured by susceptibility measurements (Ref. 55) and the average E_{2g} phonon frequency.

experimental data and the theoretical predictions. The data show a relevant softening occurring only at $x=0.33$ (at the type II ETT, the opening of a neck). On the contrary theoretical calculations predict a relevant softening also at $x=0.57$ (at the type I ETT, the sigma band edge).

The intraband electron phonon coupling λ for the σ band holes has been extracted from the Raman data of the E_{2g} mode is plotted in Fig. 6(b). The electron phonon coupling has been extracted from the line-shape parameters, $\lambda=2.955\times\Gamma/\omega$, according with Ref. 11, and the softening of the E_{2g} mode, $\lambda=[(\Omega/\omega)-1]3/4$ according with Ref. 15. In Fig. 6(b) we plot the calculated effective electron-phonon coupling $\lambda^*=[\lambda/(1+\lambda)]$ determined from phonon softening and phonon broadening. The value of the coupling extracted from the E_{2g} phonon frequency and linewidth roughly agree. These results are compared with the experimental measure of the effective experimental coupling $\tilde{\lambda}_{exp}=-\ln(K_BT_c/\hbar\omega_{E_{2g}})$ obtained from the experimental T_c and average phonon E_{2g} frequency. The McMillan's equation $\tilde{\lambda}_{exp}=(\lambda^*-\mu^*)$ where μ^* is the effective Coulomb repulsion is valid for $\lambda<1.25$. In the range $0<x<0.25$ $\lambda^*>\tilde{\lambda}_{exp}$ *so that* $\mu^*>0$ therefore a phonon mediated pairing is possible and the effective Coulomb repulsion decreases with x up to reach zero for $x=0.3$. On the contrary for higher Al substitution, $x>0.25$, where $\lambda^*<\tilde{\lambda}_{exp}$ the electron-phonon coupling cannot give account of the actual critical temperature (it will require an attractive Coulomb pseudopotential). In this range the measured critical temperature is considerably higher than the one calculated on the basis of the variation of the intraband e-ph coupling in the σ band. Therefore the results reported here suggest that the intraband el-ph coupling seems not to be the only driving mechanism for high T_c in the $Mg_{1-x}Al_xB_2$ system and support a joint role of an electronic or exchangelike pairing mechanism.

IV. CONCLUSION

In conclusion we have reported the micro-Raman study of the boron isotope effect on the E_{2g} phonon mode in $Mg_{1-x}Al_xB_2$ system in a wide range of Al content ($0<x<0.57$). We have found that the isotope coefficient of the E_{2g} phonon mode follows the normal mass law for most of the Al content. Only at very low Al concentration the phonon isotope coefficient $\alpha\sim0.4-0.3$ deviate slightly from the harmonic mass law.

In agreement with previous work[2,33] we have detected the mesoscopic phase separation that occurs in this system near the electronic topological transition of the Fermi surface in the presence of impurities. It is interesting to underline the coexistence in this system of different structural phases while the superconducting phase shows a single superconducting T_c similarly to other high T_c superconductor.

Moreover we have reported the measured softening and widening of the E_{2g} mode, i.e., the Kohn anomaly at the electronic topological transition from a 3D to a 2D Fermi surface in the isotopically pure samples. From the softening and the widening of the E_{2g} mode we have calculated the electron-phonon coupling for increasing Al concentration. The comparison of the E_{2g} experimental softening with theoretical predictions[52,53,59] show large disagreement. The effective electron phonon coupling deduced from transport and Raman data, within the standard BCS scheme, decreases much more slowly with x than the effective electron phonon coupling variation with x, deduced from the Khon anomaly on the phonon spectrum.

Finally we think that these results support the idea that a strong electron-phonon coupling in the σ band giving bipolaronlike pairs for $0<x<0.3$ coexist the exchangelike pairing mechanism between pairs in the σ band and in the π band. It is possible that this nonstandard BCS mechanism, involving exchangelike pairing in anisotropic multigap superconductors and in the diborides,[31] is the driving mechanism for high T_c superconductivity also in other quite different materials: cuprate perovskites[60–63] and in the recently discovered iron pnictides (or FeAs multilayer) superconductors.[8,9] The convergence toward this unitary scenario for the pairing mechanism in high T_c superconductors is based on the common features[64–70] appearing in quite different systems. We have shown here that diborides share, with other high T_c superconductors, the typical feature of being in a region near the edge of phase separation. It is possible that this is at the quantum critical point of a first order phase transition[3,9,68] driven by two variables, first, the electronic doping in the active planes and, second, the elastic misfit strain between the planes in the multilayer.

ACKNOWLEDGMENTS

Thanks are due to Robert Markiewicz for very useful discussions. This work is the result of an European scientific collaboration focused on "Controlling Mesoscopic Phase Separation" (COMEPHS) in advanced functional materials supported by the European STREP Project No. 517039.

[1] S. Agrestini, D. Di Castro, M. Sansone, N. L. Saini, A. Saccone, S. De Negri, M. Giovannini, M. Colapietro, and A. Bianconi, J. Phys.: Condens. Matter **13**, 11689 (2001) and references therein.
[2] V. Palmisano, L. Simonelli, A. Puri, M. Fratini, Y. Busby, P. Parisiades, E. Liarokapis, M. Brunelli, A. N. Fitch, and A. Bianconi, J. Phys.: Condens. Matter **20**, 434222 (2008) and references therein.
[3] A. Bianconi, G. Bianconi, S. Caprara, D. Di Castro, H. Oyanagi, and N. L. Saini, J. Phys.: Condens. Matter **12**, 10655 (2000).
[4] M. Fratini, N. Poccia, and A. Bianconi, J. Phys.: Conf. Ser. **108**, 012036 (2008).
[5] A. Bianconi, Int. J. Mod. Phys. B **14**, 3289 (2000); N. L. Saini and A. Bianconi, *ibid.* **14**, 3649 (2000).
[6] K. I. Kugel, A. L. Rakhmanov, A. O. Sboychakov, N. Poccia, and A. Bianconi, Phys. Rev. B **78**, 165124 (2008) and references therein.
[7] A. Bianconi, J. Supercond. **18**, 25 (2005) and references therein.
[8] M. Fratini, R. Caivano, A. Puri, A. Ricci, Z.-A. Ren, Xiao-Li Dong, Jie Yang, Wei Lu, Zhong-Xian Zhao, L. Barba, G. Arrighetti, M. Polentarutti, and A. Bianconi, Supercond. Sci. Technol. **21**, 092002 (2008).
[9] R. Caivano, M. Fratini, N. Poccia, A. Ricci, A. Puri, Z.-A. Ren, X.-L. Dong, J. Yang, W. Lu, Z.-X. Zhao, L. Barba, and A. Bianconi, Supercond. Sci. Technol. **22**, 014004 (2009).
[10] I. M. Lifshitz, Sov. Phys. JETP **11**, 1130 (1960).
[11] W. E. Pickett, Braz. J. Phys. **33**, 695 (2003).
[12] S. L. Bud'ko, G. Lapertot, C. Petrovic, C. E. Cunningham, N. Anderson, and P. C. Canfield, Phys. Rev. Lett. **86**, 1877 (2001).
[13] D. G. Hinks and J. D. Jorgensen, Physica C **385**, 98 (2003).
[14] Y. Kong, O. V. Dolgov, O. Jepsen, and O. K. Andersen, Phys. Rev. B **64**, 020501(R) (2001).
[15] L. Boeri, J. Kortus, and O. K. Andersen, Phys. Rev. Lett. **93**, 237002 (2004).
[16] I. I. Mazin and V. P. Antropov, Physica C **385**, 49 (2003).
[17] T. Yildirim, O. Gülseren, J. W. Lynn, C. M. Brown, T. J. Udovic, Q. Huang, N. Rogado, K. A. Regan, M. A. Hayward, J. S. Slusky, T. He, M. K. Haas, P. Khalifah, K. Inumaru, and R. J. Cava, Phys. Rev. Lett. **87**, 037001 (2001).
[18] M. Calandra, M. Lazzeri, and F. Mauri, Physica C **456**, 38 (2007).
[19] A. S. Alexandrov, Physica C **363**, 231 (2001).
[20] G. Baskaran, Phys. Rev. B **65**, 212505 (2002).
[21] J. Hirsch, Phys. Lett. A **282**, 392 (2001).
[22] S. G. Sharapov, V. P. Gusynin, and H. Beck, Eur. Phys. J. B **30**, 45 (2002).
[23] D. Varshney, M. S. Azad, and R. K. Singh, Supercond. Sci. Technol. **17**, 1446 (2004).
[24] D. Varshney and M. Nagar, Supercond. Sci. Technol. **20**, 930 (2007).
[25] K. Voelker, V. I. Anisimov, and T. M. Rice, arXiv:cond-mat/0103082 (unpublished).
[26] A. Balassis, E. V. Chulkov, P. M. Echenique, and V. M. Silkin, Phys. Rev. B **78**, 224502 (2008).
[27] M. Imada, J. Phys. Soc. Jpn. **70**, 1218 (2001).
[28] K. Yamaji, J. Phys. Soc. Jpn. **70**, 1476 (2001); I. Hase and K. Yamaji, *ibid.* **70**, 2376 (2001).
[29] T. Örd and N. Kristoffel, Physica C **370**, 17 (2002); N. Kristoffel, T. Örd, and K. Rago, Europhys. Lett. **61**, 109 (2003).
[30] A. Bianconi, D. Di Castro, S. Agrestini, G. Campi, N. L. Saini, A. Saccone, S. De Negri, and M. Giovannini, J. Phys.: Condens. Matter **13**, 7383 (2001).

[31] A. Bussmann-Holder and A. Bianconi, Phys. Rev. B **67**, 132509 (2003).
[32] G. A. Ummarino, R. S. Gonnelli, S. Massidda, and A. Bianconi, Physica C **407**, 121 (2004).
[33] A. F. Goncharov and V. V. Struzhkin, Physica C **385**, 117 (2003).
[34] J. S. Slusky, N. Rogado, K. A. Regan, M. A. Hayward, P. Khalifah, T. He, K. Inumaru, S. M. Loureiro, M. K. Haas, H. W. Zandbergen, and R. J. Cava, Nature (London) **410**, 343 (2001).
[35] A. Bianconi, S. Agrestini, D. Di Castro, G. Campi, G. Zangari, N. L. Saini, A. Saccone, S. De Negri, M. Giovannini, G. Profeta, A. Continenza, G. Satta, S. Massidda, A. Cassetta, A. Pifferi, and M. Colapietro, Phys. Rev. B **65**, 174515 (2002).
[36] H. W. Zandbergen, M. Y. Wu, H. Jiang, M. A. Hayward, M. K. Haas, and R. J. Cava, Physica C **366**, 221 (2002).
[37] H. Luo, C. M. Li, H. M. Luo, and S. Y. Ding, J. Appl. Phys. **91**, 7122 (2002).
[38] J. Y. Xiang, D. N. Zheng, J. Q. Li, S. L. Li, H. H. Wen, and Z. X. Zhao, Physica C **386**, 611 (2003).
[39] M. Putti, C. Ferdeghini, M. Monni, I. Pallecchi, C. Tarantini, P. Manfrinetti, A. Palenzona, D. Daghero, R. S. Gonnelli, and V. A. Stepanov, Phys. Rev. B **71**, 144505 (2005).
[40] B. Birajdar, T. Wenzel, P. Manfrinetti, A. Palenzona, M. Putti, and O. Eibl, Supercond. Sci. Technol. **18**, 572 (2005).
[41] A. J. Zambano, A. R. Moodenbaugh, and L. D. Cooley, Supercond. Sci. Technol. **18**, 1411 (2005).
[42] J. Karpinski, N. D. Zhigadlo, G. Schuck, S. M. Kazakov, B. Batlogg, K. Rogacki, R. Puzniak, J. Jun, E. Müller, P. Wägli, R. Gonnelli, D. Daghero, G. A. Ummarino, and V. A. Stepanov, Phys. Rev. B **71**, 174506 (2005).
[43] P. Samuely, P. Szabo´, P. C. Canfield, and S. L. Bud'ko, Phys. Rev. Lett. **95**, 099701 (2005).
[44] L. D. Cooley, A. J. Zambano, A. R. Moodenbaugh, R. F. Klie, Jin-Cheng Zheng, and Yimei Zhu, Phys. Rev. Lett. **95**, 267002 (2005).
[45] R. F. Klie, J. C. Zheng, Y. Zhu, A. J. Zambano, and L. D. Cooley, Phys. Rev. B **73**, 014513 (2006).
[46] S. Tsuda, T. Yokoya, T. Kiss, T. Shimojima, S. Shin, T. Togashi, S. Watanabe, C. Zhang, C. T. Chen, S. Lee, H. Uchiyama, S. Tajima, N. Nakai, and K. Machida, Phys. Rev. B **72**, 064527 (2005); S. Tsuda, T. Yokoya, T. Kiss, T. Shimojima, S. Shin, T. Togashi, S. Watanabe, C. Q. Chang, C. Chen, S. Lee, H. Uchiyama, S. Tajima, N. Nakai, and K. Machida, Physica C **460-462**, 80 (2007).
[47] R. S. Gonnelli, D. Daghero, G. A. Ummarino, M. Tortello, D. Delaude, V. A. Stepanov, and J. Karpinski, Physica C **456**, 134 (2007).
[48] P. Postorino, A. Congeduti, P. Dore, A. Nucara, A. Bianconi, D. Di Castro, S. De Negri, and A. Saccone, Phys. Rev. B **65**, 020507(R) (2001).
[49] D. Di Castro, S. Agrestini, G. Campi, A. Cassetta, M. Colapietro, A. Congeduti, A. Continenza, S. De Negri, M. Giovannini, S. Massidda, M. Nardone, A. Pifferi, P. Postorino, G. Profeta, A. Saccone, N. L. Saini, G. Satta, and A. Bianconi, Europhys. Lett. **58**, 278 (2002).
[50] B. Renker, K. B. Bohnen, R. Heid, D. Ernst, H. Schober, M. Koza, P. Adelmann, P. Schweiss, and T. Wolf, Phys. Rev. Lett. **88**, 067001 (2002).
[51] J. Kortus, Oleg V. Dolgov, R. K. Kremer, and A. A. Golubov, Phys. Rev. Lett. **94**, 027002 (2005).
[52] G. Profeta, A. Continenza, and S. Massidda, Phys. Rev. B **68**, 144508 (2003).
[53] P. Zhang, S. G. Louie, and M. L. Cohen, Phys. Rev. Lett. **94**, 225502 (2005).
[54] H. D. Yang, H. L. Liu, J.-Y. Lin, M. X. Kuo, P. L. Ho, J. M. Chen, C. U. Jung, Min-Seok Park, and Sung-Ik Lee, Phys. Rev. B **68**, 092505 (2003).
[55] A. Bianconi, Y. Busby, M. Fratini, V. Palmisano, L. Simonelli, M. Filippi, S. Sanna, F. Congiu, A. Saccone, M. Giovannini, and S. De Negri, J. Supercond. Novel Magn. **20**, 495 (2007).
[56] O. de la Peña, A. Aguayo, and R. de Coss, Phys. Rev. B **66**, 012511 (2002).
[57] O. De la Peña-Seaman, R. de Coss, R. Heid, and K.-P. Bohnen, Phys. Rev. B **76**, 174205 (2007).
[58] S. Agrestini, C. Metallo, M. Filippi, L. Simonelli, G. Campi, C. Sanipoli, E. Liarokapis, S. De Negri, M. Giovanni, A. Saccone, A. Latini, and A. Bianconi, Phys. Rev. B **70**, 134514 (2004).
[59] O. De la Peña-Seaman, R. de Coss, R. Heid, and K.-P. Bohnen, Phys. Rev. B **79**, 134523 (2009).
[60] A. Bianconi, N. L. Saini, S. Agrestini, D. Di Castro, and G. Bianconi, Int. J. Mod. Phys. B **14**, 3342 (2000).
[61] D. Di Castro, M. Colapietro, and G. Bianconi, Int. J. Mod. Phys. B **14**, 3438 (2000).
[62] A. Bianconi, S. Agrestini, G. Bianconi, D. Di Castro, and N. L. Saini, J. Alloys Compd. **317-318**, 537 (2001).
[63] S. Agrestini, N. L. Saini, G. Bianconi, and A. Bianconi, J. Phys. A **36**, 9133 (2003).
[64] A. Bianconi, S. Agrestini, G. Campi, M. Filippi, and N. L. Saini, Curr. Appl. Phys. **5**, 254 (2005).
[65] J. Annett, F. Kusmartsev, and A. Bianconi, Supercond. Sci. Technol. **22**, 010301 (2009).
[66] A. Bianconi, N. Poccia, and A. Ricci, J. Supercond. Novel Magn. **22**, 527 (2009).
[67] N. Poccia and M. Fratini, J. Supercond. Novel Magn. **22**, 299 (2009).
[68] Y. J. Uemura, Nature Mater. **8**, 253 (2009).
[69] Jan Zaanen, Nature (London) **457**, 546 (2009).
[70] S. A. Kivelson and H. Yao, Nature Mater. **7**, 927 (2008).